The effect of adding CsCl content on physicochemical properties of (GeS2–Sb2S3)100-x(CsCl)x (0 ≤ x ≤ 40 mol%) chalcohalide glasses

Imed Boukhris (imed_boukhris@yahoo.fr)
King Khalid University

Imen Kebaili
King Khalid University

Research Article

Keywords: Chalcohalide glasses, chemical bond approach, physico-chemical properties, band-gap engineering, glass-transition temperature

Posted Date: March 31st, 2021

DOI: https://doi.org/10.21203/rs.3.rs-361864/v1

The effect of adding CsCl content on physicochemical properties of $(GeS_2–Sb_2S_3)_{100-x}(CsCl)_x$ ($0 \leq x \leq 40$ mol%) chalcohalide glasses

Imed Boukhris[a,b] and Imen Kebaili[a,c*]

[a]Department of Physics, Faculty of Science, King Khalid University; P.O. Box 9004, Abha, Saudi Arabia.
[b]Université de Sfax, Faculté des Sciences de Sfax, Département de Physique, Laboratoire des matériaux composites céramiques et polymères (LaMaCoP) BP 805, Sfax 3000, Tunisie
[c]Laboratoire de Physique Appliquée, Groupe des Matériaux Luminescents, Université de Sfax, Faculté des Sciences de Sfax, BP 1171, 3000 Sfax, Tunisia[2]

Abstract

The physico-chemical properties of $(GeS_2–Sb_2S_3)_{100-x}(CsCl)_x$ ($0 \leq x \leq 40$ mol%) chalcohalide glasses were theoretically studied. The band gap (E_g) of the studied glass system was estimated and was found to increase by adding the CsCl content. Furthermore, the positions of the valence band and conduction band edges was determined. The results reveal that the molar volume (V_m) of the studied samples increased while the density (ρ) and the number of atoms per unit volume (N) decreased with increasing the CsCl content. The overall coordination number (CN), constraints number (N_s) and overall mean bond energy (<E>) were computed using the chemical bond approach and were found to decrease. In contrast, the number of lone-pair electrons (LP) and cohesive energy (CE) increased. Finally, the glass-transition temperature (T_g) was also estimated based on the overall mean bond energy, and was found to decrease with increasing the CsCl content.

Keywords: Chalcohalide glasses, chemical bond approach, physico-chemical properties, band-gap engineering, glass-transition temperature

*Corresponding author email: imen_kbb@yahoo.fr

1. Introduction

Chalcogenide glasses (ChGs) are attractive research subjects owing to their exceptional properties like high refractive index, wide transparency and low photon energy, and are used in various applications, including in the radiation shielding field, infrared optics, optical amplifiers, optical sensors, and nonlinear optics [1–4]. The properties of these ChGs were frequently investigated. Dahshan *et al.* [5] studied the optical constants of Ge-Sb-Se-I chalcogenide glasses via a single reflectance spectrum. They proved that the refractive index and the Urbach energy increase while the optical band gap decreases by adding the iodine content. Aly *et al.* [6] studied the ternary $Cu_x(Ge_{30}Se_{70})_{100-x}$ thin films in terms of optical constants. The main result showed that the optical band gap decreases whereas Urbach energy increases by increasing Cu content. Mehta *et al* [7] investigated the effect of tellurium addition on the physicochemical properties of $Ge_{10}Se_{90-x}Te_x$ glassy alloy. The authors showed that the density, molar volume and compactness of the samples increase whereas the optical band gap decreases with the addition of Te amount. Nevertheless, ChGs have some drawbacks, such as their reduced thermal and mechanical properties, which limit their uses [8]. Hence, it is crucial to improve these properties for better applications by making compositional changes. Many recent studies have shown that adding metal halides to the glass matrices overcomes the high coefficient of thermal expansion as well as low fracture toughness of glasses, which eliminate the drawbacks that prevent the intensive use of ChGs in infrared (IR) optical and photonic fields [9, 10]. Therefore, ChGs containing metal halides, named chalcohalide glasses, have become a very attractive research topic in many domains. They not only retain the exceptional IR optical properties and are low cost to synthesise, but also enhance the chemical stability and thermomechanical properties of glasses [12-14]. These properties are highly dependent on the glass matrix composition and the amount and kind of metal halide existing in the glass matrix [15]. In this context, many researchers have investigated the impact of adding CsCl metal halide to Ge-Sb-S ChGs and extracted results for various aspects. Yang *et al.* investigated the impact of annealing temperature on the properties of Ge–Sb–S–CsCl ChGs [16]. Their results indicate that rigorous control of the annealing process is crucial for creating chalcohalides with enhanced mechanical properties and reduced optical loss. Hao *et al.* described the

fabrication and microstructure of Ge–Sb–S–CsCl ChGs [17]. The principal result was that these glasses had higher transmittance in the far and mid IR spectral region. Delaisir *et al.* synthesised GeS_2–Sb_2S_3–CsCl chalcohalide glasses with finely porous surfaces [10]. They showed that porous ChGs can be used as optical elements in an attenuated total reflectance (ATR) configuration.

For better applying chalcohalide glasses, one of the main points is to investigate their physico-chemical properties in terms of overall coordination number, overall cohesive energy, overall mean bond energy, distribution and strength of chemical bonds, etc. Indeed, properties of glasses are highly affected by these characteristics. However, the above-mentioned researches show that no study has been published to date on the physical and chemical properties of GeS_2–Sb_2S_3–CsCl chalcohalide glasses. Therefore, the present study focuses on a detailed investigation of the physico-chemical properties of chalcohalide glasses with the composition $(GeS_2–Sb_2S_3)_{100-x}(CsCl)_x$. In particular, the effect of adding CsCl on the physico-chemical, optical and thermal properties of this glassy system was investigated. The distribution and strength of the chemical bonds in the studied system were determined with the help of the chemical bond approach (CBA) [18]. These data were then used to compute the average coordination number, constraints number, cohesive energy, lone-pair electrons and mean bond energy. Furthermore, different estimations of the band gap and positions of the conduction band and valence band edges were presented. An estimation of the glass-transition temperature was also presented.

2. Results and discussion

To elucidate the correlation between optical and physico-chemical properties, the optical band gap energy (E_g) of $(GeS_2–Sb_2S_3)_{100-x}(CsCl)_x$ (x = 0, 5, 10, 15, 20, 25, 30, 35 and 40 mol%) chalcohalide glasses has to be estimated first. For this system, E_g can be estimated theoretically by different methods.

The first estimation expressed E_g as a function of the density (ρ) of the chalcohalide glass system by a simple empirical equation [19]:

$$E_{g1} = E_0 - a.\rho \quad (1)$$

where $E_0 = 4.5 \pm 0.1$eV and $a = 0.65 \pm 0.01$eV.cm^3/g.

The densities used were measured by Zhao *et al.* for the same $(GeS_2–Sb_2S_3)_{100-x}(CsCl)_x$ glassy system [20]. The calculated values of E_{g1} and measured densities are listed in Table 1.

Using the chemical bond approach (CBA) [18], the distribution of the chemical bonds was estimated and a second estimation of the compound's band gap was made as [21]:

$$E_{g2} = P_{Cs-Cl}.E_g(CsCl) + P_{Ge-S}.E_g(GeS_2) + P_{Sb-S}.E_g(Sb_2S_3) + P_{Sb-Sb}.E_g(Sb) \quad (2)$$

$P_{Cs–Cl}$, $P_{Ge–S}$, $P_{Sb–S}$ and $P_{Sb–Sb}$ are the percentages of the corresponding bonds (see Table 1), and $E_g(CsCl)$, $E_g(GeS_2)$, $E_g(Sb_2S_3)$ and $E_g(Sb)$ are 5.46eV [22], 2.35eV [23], 1.73eV [24] and 0.15 [25], respectively. This method takes into account the surroundings of each atom as predicted by CBA. When calculating the bond's percentages, we assumed, according to CBA, that heteropolar bonds with higher energy were formed first. Another basic assumption of CBA is that homopolar bonds occur after the formation of all possible heteropolar bonds. The calculated E_{g2} values and the chemical bond's proportion are summarised in Table 1.

Table 1 clearly shows that E_{g1} and E_{g2} agree quantitatively and qualitatively. Indeed, both E_{g1} and E_{g2} increased linearly. Hence the arithmetic average of E_{g1} and E_{g2} could be a good approximation of the optical band gap.

$$E_g = \frac{E_{g1}+E_{g2}}{2} \quad (3)$$

Figure 1 plots E_g against the CsCl content. This figure shows that E_g increased from 2.08 eV to 2.42 eV when the CsCl content increased from 0 to 40 mol%. Thus, the studied glasses may be suitable for optical absorption in the wavelength range between 0.51 and 0.59μm, which makes them suitable for a variety of applications including solar cells.

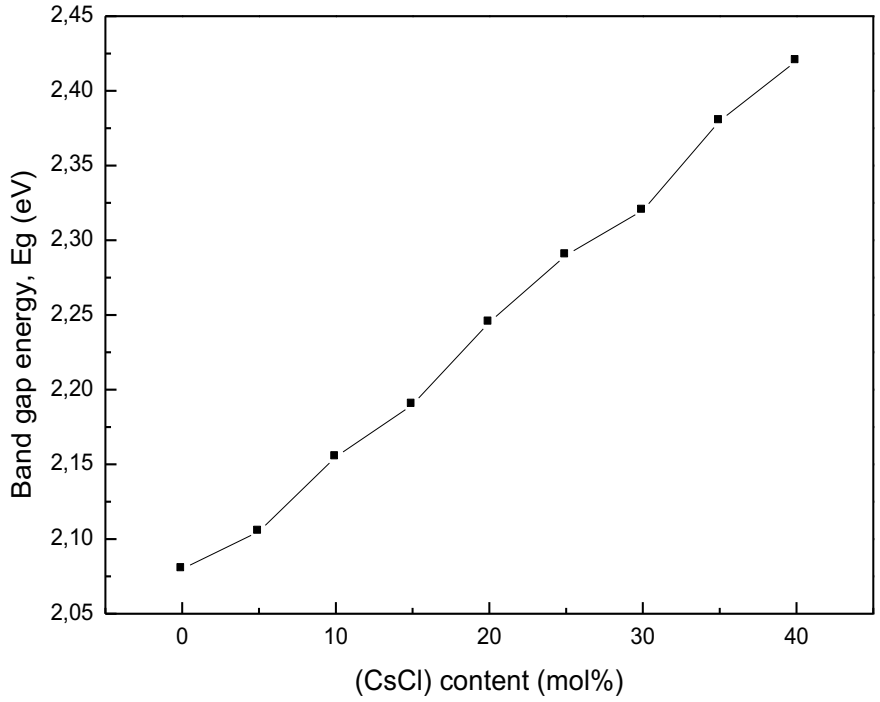

Fig.1. Band gap estimation for $(GeS_2\text{-}Sb_2S_3)_{100-x}(CsCl)_x$ system

Table. 1. Density, chemical bond's distribution and optical band gap estimations for the $(GeS_2\text{-}Sb_2S_3)_{100-x}(CsCl)_x$ system

***x* (mol%)**	***ρ*** **(g/cm³) [20]**	**Chemical bond's distribution (%)**				**Theoretically calculated Eg (eV)**		
		$P_{Cs\text{-}Cl}$	**$P_{Ge\text{-}S}$**	**$P_{Sb\text{-}S}$**	**$P_{Sb\text{-}Sb}$**	**Eg_1**	**Eg_2**	**Eg**
0	3.67	0	0.524	0.476	0	2.11	2.05	2.08
5	3.66	0.021	0.502	0.461	0.016	2.12	2.09	2.1
10	3.56	0.043	0.479	0.444	0.034	2.18	2.13	2.15
15	3.52	0.067	0.453	0.427	0.053	2.21	2.17	2.19
20	3.42	0.092	0.422	0.413	0.073	2.27	2.22	2.24
25	3.37	0.12	0.393	0.393	0.096	2.31	2.27	2.29
30	3.35	0.15	0.36	0.37	0.12	2.32	2.32	2.32
35	3.26	0.184	0.324	0.345	0.147	2.38	2.38	2.38
40	3.23	0.217	0.283	0.326	0.174	2.4	2.44	2.42

Estimation of the positions of the conduction band and valence band (E_{CB} and E_{VB}, respectively) is important for manufacturing semiconductor devices. E_{CB} and E_{VB} (in eV) values are calculated from E_g values (see table 1), ionisation energy (E_{Ion}) and electron affinity (E_{EA}). E_{CB} and E_{VB} for $(GeS_2–Sb_2S_3)_{100-x}(CsCl)_x$ system were determined as follows [26–29]:

$$E_{CB} = E_C - X + \frac{E_g}{2} \quad \text{and} \quad E_{VB} = E_C - X - \frac{E_g}{2} \tag{4}$$

$$\text{Where } X = [(X_{Ge})^{MF_{Ge}}.(X_S)^{MF_S}.(X_{Sb})^{MF_{Sb}}.(X_{Cs})^{MF_{Cs}}.(X_{Cl})^{MF_{Cl}}] \tag{5}$$

where E_C = 4.5 eV [26, 27].

Using the E_{EA} and E_{ION} of the elements (see Table 2), we obtained X_{Ge}, X_S, X_{Sb}, X_{Cs}, X_{Cl} and X. Table 3 regroups the computed values for X, E_{CB} and E_{VB}.

Table.2. Elements' properties used for calculation

	CN	BE(kcal/mol)	χ [30]	Aw [30]	E_{EA} [30]	E_{ION} [30]
Ge	4 [31-33]	37.6 [25, 33]	2.01	72.64	1.235	7.910
S	2 [35]	50.9 [35]	2.58	32.065	2.077	10.36
Sb	3 [25]	30.22 [25]	2.05	121.76	1.071	8.657
Cs	1 [30]	10.5 [30]	0.79	132.905	0.471	3.893
Cl	1 [30]	58.07 [30]	3.16	35.4527	3.614	13.014

Table.3. X, E_{CB} and E_{VB} for the $(GeS_2\text{-}Sb_2S_3)_{100-x}(CsCl)_x$ system

x (mol%)	X	E_{CB}	E_{VB}
		(eV)	
0	5.624	-0.082	-2.166
5	5.557	-0.004	-2.111
10	5.491	0.088	-2.07
15	5.425	0.171	-2.022
20	5.36	0.262	-1.984
25	5.296	0.347	-1.941
30	5.233	0.427	-1.895
35	5.171	0.519	-1.862
40	5.109	0.601	-1.819

Figure 2 shows the plots of E_{CB} and E_{VB}. Although both E_{CB} and E_{VB} increased with increasing CsCl content in the $(GeS_2–Sb_2S_3)_{100-x}(CsCl)_x$ system, the increase in E_{CB} was more pronounced, which explains the increase in E_g previously observed.

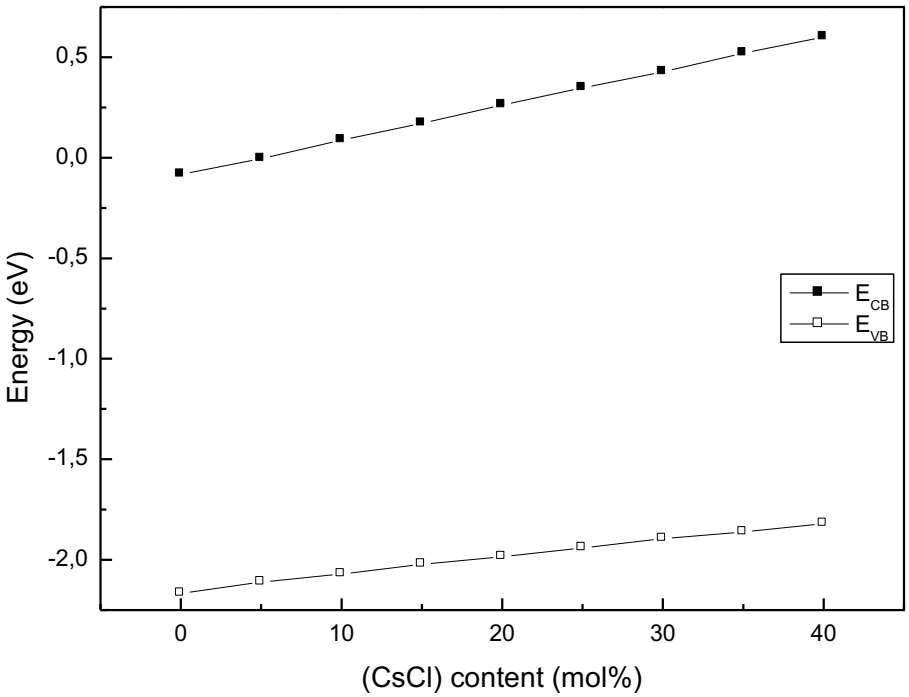

Fig.2. Plots of E_{CB} and E_{VB} against the (CsCl) content for the $(GeS_2\text{-}Sb_2S_3)_{100-x}(CsCl)_x$ system

Table 1 shows that increasing the CsCl content led to a decrease in density which accounts for the increase in the optical band gap. To confirm this result, we calculated molar volume from the density values cited in Table 1 as:

$$V_m = \rho^{-1} \sum_i x_i Aw_i \quad (6)$$

where x_i and Aw_i are the atomic percent and the atomic weight of the i^{th} element listed in Table 2. V_m values are listed in Table 4. The variation in V_m with composition is plotted in Figure 3 which clearly shows that V_m increased from 15.46 to 19.99 cm^3/mol as the CsCl content increased from 0 to 40%. We note that E_g (see Fig. 1) and V_m had the same increasing trend. This effect was also shown in previous studies [36].

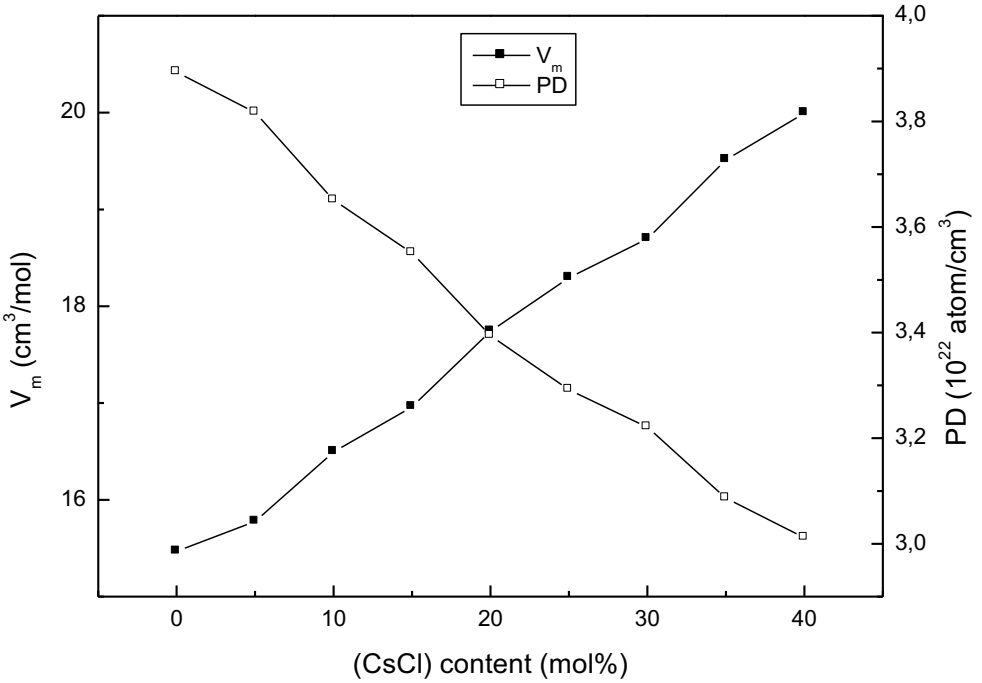

Fig.3. Plots of V_m and PD against the (CsCl) content for the $(GeS_2\text{-}Sb_2S_3)_{100\text{-}x}(CsCl)_x$ system

Table.4. Theoretical computation of some parameters for the $(GeS_2\text{-}Sb_2S_3)_{100\text{-}x}(CsCl)_x$ system

X (mol %)	V_m (cm^3/mol)	PD (10^{22} atm/cm^3)	R	CN	Ns	LP	$\Delta\chi$	CE (kca/mol)	<E> (eV)
0	15.46	3.893	1	2.53	3.33	2.93	0.551	63.89	2.786
5	15.77	3.817	0.989	2.44	3.11	2.95	0.579	64.74	2.776
10	16.49	3.651	0.979	2.35	2.89	2.98	0.609	65.6	2.765
15	16.96	3.551	0.967	2.27	2.67	3.01	0.642	66.45	2.754
20	17.74	3.394	0.955	2.18	2.45	3.03	0.676	67.78	2.741
25	18.29	3.291	0.942	2.09	2.24	3.05	0.715	68.64	2.727
30	18.69	3.221	0.928	2.01	2.02	3.08	0.756	69.49	2.711
35	19.51	3.086	0.912	1.92	1.8	3.11	0.802	70.34	2.695
40	19.99	3.011	0.896	1.83	1.58	3.13	0.849	71.67	2.677

In ChGs, the conduction band edge energy is decided by the number of atoms per unit volume [37]. Therefore, packing density (PD) was calculated as the ratio of used space to the allocated space [38]:

$$PD = \frac{N_a \cdot \rho}{M} \tag{7}$$

where N_a and M are Avogadro's number and molecular weight, respectively. Calculated PD values are cited in Table 4.

The molecular weight of CsCl is greater than those of GeS_2 and Sb_2S_3; due to this, PD decreased while V_m increased as the proportion of CsCl in the glassy system increased (see Fig. 3) [38].

The increase in V_m and the decrease in PD led to a rise in the energy of the conduction band edge, which corresponded to an increase in the optical gap [37]. All the aforementioned results confirm the increase in E_g and the variation in E_{CB} and E_{VB} positions shown in Figure 1 and Figure 2, respectively, and highlight the very close correlation between optical and physico-chemical properties.

Using the coordination numbers of the elements listed in Table 2, we calculated the overall CN for the $(GeS_2–Sb_2S_3)_{100-x}(CsCl)_x$ chalcohalide glasses as follows:

$$CN = CN_{Ge}.MF_{Ge} + CN_S.MF_S + CN_{Sb}.MF_{Sb} + CN_{Cs}.MF_{Cs} + CN_{Cl}.MF_{Cl} \quad (8)$$

where MF_{Ge}, MF_S, MF_{Sb}, MF_{Cs}, and MF_{Cl} are the mole fractions for Ge, S, Sb, Cs and Cl, respectively.

The constraints number (N_s), which represents the rigidity of glasses, was computed using the CN values [39]:

$$N_s = \frac{CN}{2} + (2CN - 3) \quad (9)$$

The computed CN and N_s values for the $(GeS_2–Sb_2S_3)_{100-x}(CsCl)_x$ glassy system are given in Table 4. Figure 4 shows the variation in CN and N_s with increasing the CsCl content. Indeed, when there was no added CsCl content, the first composition was stressed–rigid or over-coordinated since CN > 2.4 and N_s > 3 (these two values are known as the rigidity percolation threshold) according to constraint theory [40]. The second composition (5 mol% of CsCl) was the optimally coordinated or ideal glass since CN and N_s were almost equal to 2.4 and 3, respectively. When further increasing CsCl content (≥ 10 mol %), CN and N_s dramatically decreased, and the compositions became floppy or under-coordinated glasses with CN < 2.4 and N_s < 3. This decrease is a sign of the diminishing rigidity of the glasses. This aspect is associated with decreased cross-linkage because of the substitution of GeS_2 and Sb_2S_3, which have higher coordination numbers (CN_{GeSe2} = 2.66 and CN_{Sb2Se3} = 2.4), with CsCl, which has a much lower coordination number (CN_{CsCl} = 1).

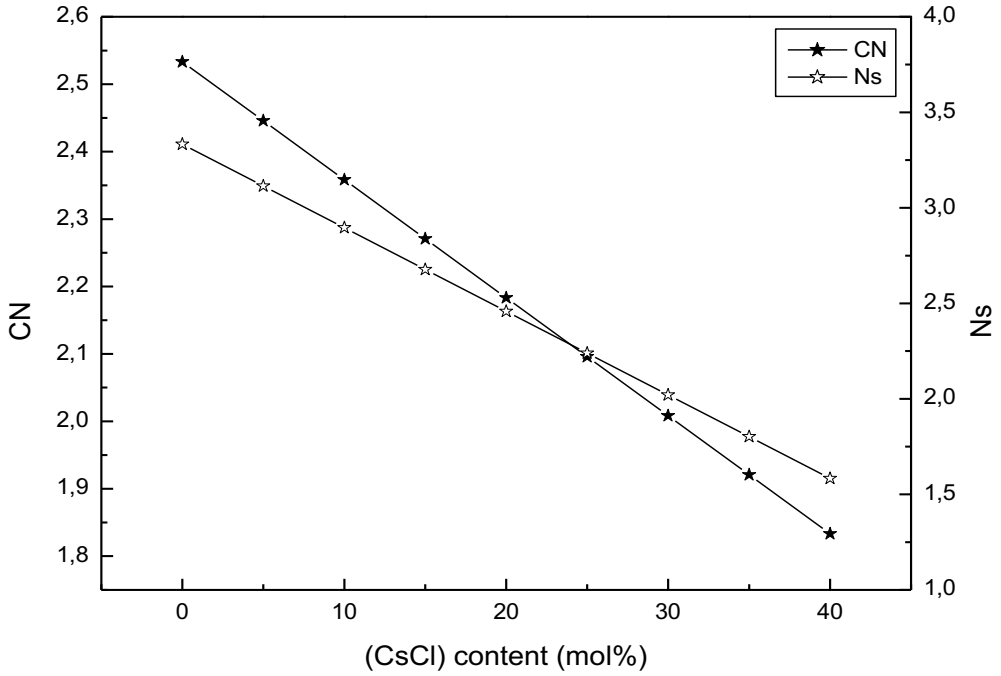

Fig.4. Plots of CN and Ns against the (CsCl) content for the $(GeS_2\text{-}Sb_2S_3)_{100\text{-}x}(CsCl)_x$ system

Philips established the concept of overall coordination number [41]. Based on this concept, Thorpe [42] introduced rigidity theory by assuming that glass is made up of rigid and floppy regions. He considered a CN value of 2.4 as the threshold for percolation of rigidity at which a transition occurs and the glass changes from floppy to rigid [43]. Thorpe estimated the floppy modes by [42]:

$$F = 2 - \frac{5}{6}CN \tag{10}$$

In Figure 5, we plot the floppy modes values against the CsCl content. An increasing trend in the floppy mode values was clearly shown, which means that the compound tended towards a floppy character as the CsCl content increased.

To explain further, the crosslinking density (CD) was calculated as [44]:

$$CD = N_s - 2 \tag{11}$$

where N_s represents the number of constraints which must be broken to attain fluidity. Figure 5 shows a clear decrease in CD values with increasing the CsCl content, which is a sign of diminishing rigidity. This confirms the previous results linked to the decrement in CN and N_s. In particular, when the CsCl content exceeded 25 mol%, CD decreased below zero; and complete transformation from a rigid to a floppy network takes place (this concentration is denoted as the percolation limit). Therefore,

incorporation of CsCl metal halide into chalcogenide systems could lead to floppy glasses. This result agrees with that of Zhang et al. who reported that adding CsCl to GeS_2–Sb_2S_3–CsCl can effectively inhibit the propagation of glass cracks [45].

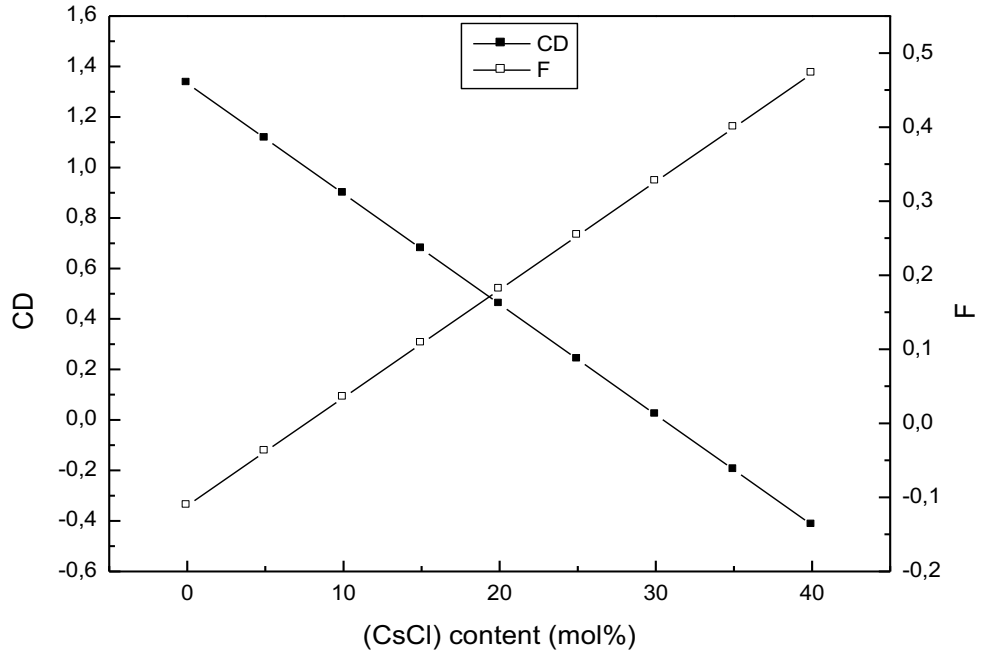

Fig.5. Plots of CD and F against the (CsCl) content for the $(GeS_2\text{-}Sb_2S_3)_{100\text{-}x}(CsCl)_x$ system

The formation of chalcogenide glass is strongly related to lone-pair electrons (LP). In fact, LP have a flexible character and can be obtained by [46]:

$$LP = VE - CN \tag{12}$$

where VE represents valence electrons.

LP values are cited in Table 4 and graphically depicted in Figure 6. It is clear that LP increased gradually with increasing CsCl content. This is caused by the rise in interaction between Ge, S and Sb atoms and lone-pair electrons of Cs and Cl atoms. The increase in LP raises bond angles flexibility which causes a decrease in the strain energy of the system [47, 48] and, consequently, leads to stable glass formation [46].

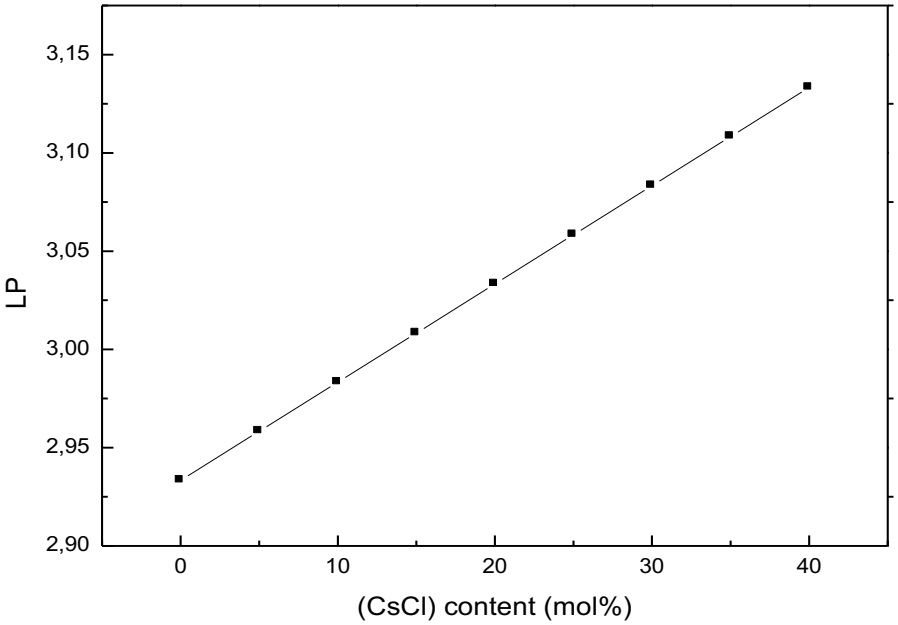

Fig.6. Variation of LP with (CsCl) content in $(GeS_2\text{-}Sb_2S_3)_{100\text{-}x}(CsCl)_x$ system

Chalcogenide glasses are characterised by deviation from stoichiometry (r) calculated as [49, 50]:

$$r = \frac{MF_S.CN_S}{MF_{Ge}.CN_{Ge}+MF_{Sb}.CN_{Sb}+MF_{Cs}.CN_{Cs}+MF_{Cl}.CN_{Cl}} \quad (13)$$

where MF_S is the molar fraction of the chalcogen atom (S) and MF_{Ge}, MF_{Sb}, MF_{Cs} and MF_{Cl} are the molar fractions of non-chalcogen atoms (Ge, Sb, Cs and Cl). According to r values (see Table 4), we conclude that the first composition is stoichiometric glass (r = 1), while the other compositions are chalcogen-poor glasses (r < 1) [46,50].

Using the homopolar bond energies (BE(i − i) and BE(j − j)) listed in Table 2, the heteropolar bond energy BE(i − j) could be estimated with the equation below [51, 52]:

$$BE(i-j) = [BE(i-i).BE(j-j)]^{1/2} + 30(\chi_i - \chi_j)^2 \quad (14)$$

where χ_i and χ_j are the electronegativities for i and j atoms, respectively.

Values for cohesive energy (CE) were obtained by summing the bond energies and are given in Table 4 [33]:

$$CE = \sum_i C_i \cdot BE_i /100 \quad (15)$$

where C_i and BE_i are the number and the energy of the bond, respectively. The chemical bond distribution was estimated using CBA and is summarised in Table 1.

Table 4 shows that CE increases with the addition of the CsCl content which confirms the increase in average stabilisation energy. The CE increase is due to the formation of Cs–Cl bonds with much higher energy compared to other bonds, BE(Cs–Cl) = 193.2 kcal/mol, BE(Ge–S) = 53.49 kcal/mol, and BE(Sb–S) = 47.64 kcal/mol (calculated using eq. 14).

The increase in E_g with increasing CsCl content (see Fig. 1) was most probably due to the higher stabilisation energy. Increased CE denotes higher bonding strength, i.e. low defect bonds. In fact, E_g is a bond-sensitive property [53]. Therefore, the increase in E_g caused by the addition of CsCl may be attributed to the increase in CE.

The majority of glassy network properties are strongly linked to the bonds formed. Therefore, the overall degree of ionicity (*Ion*) can be estimated according to Pauling for simple bonds [51]:

$$Ion = 1 - exp\left[-\frac{\Delta\chi^2}{4}\right] \quad (16)$$

where $\Delta\chi_{th}$ is the calculated overall electronegativity difference of the whole compound given as [21]:

$$\Delta\chi_{th} = P_{Cs-Cl}.|\chi(Cs) - \chi(Cl)| + P_{Ge-S}.|\chi(Ge) - \chi(S)| + P_{Sb-S}.|\chi(Sb) - \chi(S)| \quad (17)$$

The electronegativities of all elements are listed in Table 2 and the estimated values of $\Delta\chi_{th}$ are grouped in Table 4. The variation in *Ion* and $\Delta\chi$ against the CsCl content is shown in Figure 7; both $\Delta\chi$ and *Ion* increased with increasing the CsCl content. This behaviour can be attributed to the increase in excess Sb–Sb homopolar bonds (see Table 1), which decreases the degree of covalency of the compound ($Cov = \exp(-\Delta\chi^2/4)$). Consequently, the degree of iconicity increases as well as $\Delta\chi$.

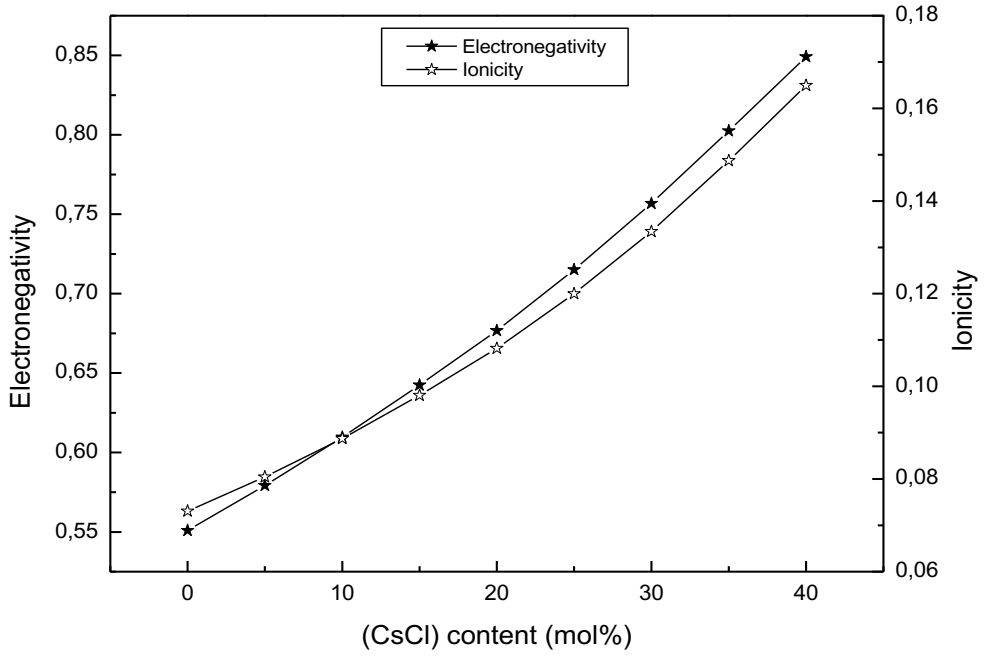

Fig.7. Plots of $\Delta\chi$ and *Ion* against the (CsCl) content for the $(GeS_2\text{-}Sb_2S_3)_{100\text{-}x}(CsCl)_x$ system

The glass-transition temperature, T_g, is the most important parameter for characterisation of the glassy state. Indeed, in terms of physical properties, T_g represents the temperature range across which the material passes from a rubbery (floppy) to a glassy (rigid) state. It is thus reasonable to suppose that the glass-transition temperature must be linked to the magnitude of cohesive forces in the network, since these forces should be surmounted to enable atom movement. Therefore, it is not surprising that predictions of T_g are generally based on simple models assuming that T_g is proportional to the mean bond energy <E>.

Tichy and Tichá, using a series of 186 glassy systems, illustrated an impressive relationship between T_g and <E> as follows [49, 50]:

$$T_g = 311.[\langle E\rangle - 0.9] \quad (18)$$

<E> is calculated as in ref. [50]:

$$\langle E\rangle = E_c + E_{rm} \quad (19)$$

A detailed discussion relating to the calculation of <E> is provided elsewhere [50]. The computed values of <E> are listed in Table 4.

Figure 8 gives the variation in T_g with the addition of CsCl content. The figure shows that T_g decreased linearly with increasing CsCl content. This decrement in T_g was

strongly correlated with the overall mean bond energy <E>. Indeed, the system was stoichiometric (r = 1) and completely cross-linked in the first composition (0% of CsCl), which thus had the highest T_g. When the CsCl content decreased, the system mean bond energy (<E>) decreased linearly leading to poor system chalcogen (r < 1), as seen in inset of figure 8. Hence, T_g diminishes due to the decreasing average bond strength. This aspect is similar in other glassy systems previously published [46].

In addition, the decrease in T_g was in perfect agreement with decreasing CN, N_s, PD and CD on the one hand and increasing V_m, LP and F on the other. Indeed, it is well known that rigidity is closely associated with T_g. These aspects were previously considered by Bocker et al. who showed that adding the CsCl metal halide into the glass matrix can cut the glass network and then decrease its rigidity [54,55].

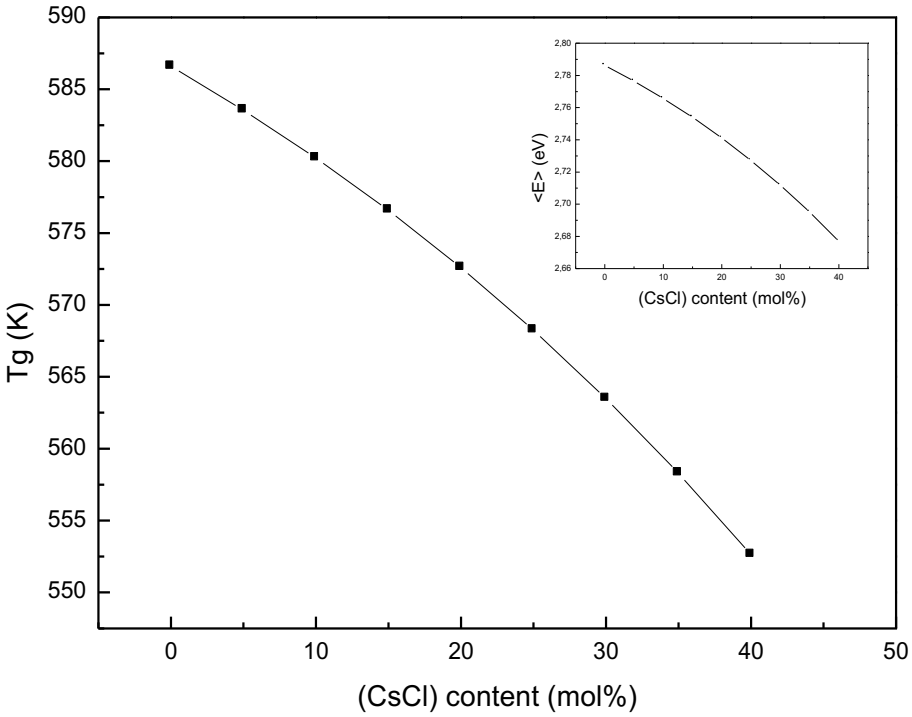

Fig.8. Variation of Tg with the (CsCl) content in the $(GeS_2\text{-}Sb_2S_3)_{100\text{-}x}(CsCl)_x$ system

3. Conclusion

The optical band gap of the $(GeS_2–Sb_2S_3)_{100\text{-}x}(CsCl)_x$ chalcohalide glasses was theoretically estimated. All estimations showed an increase in the band gap from 2.08 eV to 2.42 eV, making these glasses suitable for improvement of relevant materials operating at a wavelength between 0.51 and 0.59 μm. Thus, all compounds may be

suitable for a very wide range of applications such as solar cells. Furthermore, the positions of the valence band and the conduction band edges were theoretically determined. Using CBA, the average coordination number, constraints number and mean bond energy were computed and were found to decrease when the CsCl content increased. On the other hand, the number of lone-pair electrons and cohesive energy increased. Finally, the glass-transition temperature was estimated based on mean bond energy and was found to decrease with increasing the CsCl content.

Acknowledgement

The author gratefully thanks the Deanship of Scientific Research at King Khalid University for financial support through Research Groups Program under grant number (R.G.P1/237/42).

References

[1] I. Boukhris, M. Al-Buriahi, H. Akyildirim, A. Alalawi, I. Kebaili and M.I. Sayyed, Chalcogenide glass-ceramics for radiation shielding applications, Ceram. Inter. 46 (2020) 19385-19392.

[2] M. Bernier, V. Fortin, N. Caron, M. El-Amraoui, Y. Messaddeq and R. Vallée, Mid-infrared chalcogenide glass Raman fiber laser, J. Opt. Lett. 38 (2013) 127-129.

[3] M. Guignard, V. Nazabal, F. Smektala, J.L. Adam, O. Bohnke, C. Duverger, A. Moréac, H. Zeghlache, A. Kudlinski, G. Martinelli and Y. Quiquempois, Chalcogenide glasses based on germanium disulfide for second harmonic generation, J. Adv. Funct. Mater. 17 (2007) 3284-3294.

[4] B. Ung and M. Skorobogatiy, Extreme optical nonlinearities in chalcogenide glass fibers embedded with metallic and semiconductor nanowires, J. Appl. Phys. Lett. 99 (2011) 121102.

[5] A Dahshan, Pankaj Sharma, KA Aly, Optical constants of Ge-Sb-Se-I chalco-halide glasses using a single reflectance spectrum, Infr. Phys. & Tech. 102 (2019) 102997.

[6] KA Aly, YB Saddeek, A Dahshan, Optical constants of ternary Cux (Ge30Se70) 100-x thin films for solar cell applications, Opt. Mater. 109 (2020) 110341.

[7] P. Sharma, S.C. Katyal, Effect of tellurium addition on the physical properties of germanium selenide glassy semiconductors, Phys. B: Cond. Matt. 403 (2008) 3667-3671.

[8] S. Zhu, H.-L. Ma, M. Matecki, X. Zhang, J. Adam and J. Lucas, Controlled crystallization of GeS_2–Sb_2S_3–CsCl glass for fabricating infrared transmitting glass-ceramics, J. Non-Cryst. Sol. 351 (2005) 3309-3313.

[9] H. Ma, L. Calvez, B. Bureau, M. Le Floch, X. Zhang and L. Jacques, Crystallization study of infrared transmitting glass ceramics based on GeS_2–Sb_2S_3–CsCl, J. Phys. and Chem. of Sol. 68 (2007) 968-971.

[10] G. Delaizir, P. Lucas, X. Zhang, H. Ma, B. Bureau and J. Lucas, Infrared glass–ceramics with fine porous surfaces for optical sensor applications, J. Amer. Ceram. Soc. 90 (2007) 2073-2077.

[11] G. Delaizir, M. Dollé, P. Rozier and X.H. Zhang, Spark plasma sintering: an easy way to make infrared transparent glass–ceramics, J. Amer. Ceram. Soc. 93 (2010) 2495-2498.

[12] L. Calvez, H.-L. Ma, J. Lucas and X. Zhang, Preparation and properties of glasses and glass-ceramics based on $GeSe_2$–Sb_2Se_3 and halides, Euro. Jour. Glass. Sci. and Tech. Part B. 47 (2006) 142-145.

[13] H. Guo, H. Tao, Y. Gong and X. Zhao, Preparation and properties of chalcogenide glasses in the GeS_2–Sb_2S_3–CdS system, J. Non-Cryst. Sol. 354 (2008) 1159-1163.

[14] J.E. Shelby, Introduction to glass science and technology, Royal Society of Chemistry, 2005.

[15] G. Nagarjuna, N. Venkatramaiah, P. Satyanarayana and N. Veeraiah, Fe_2O_3-induced crystallization and the physical properties of lead arsenate glass system, J. Allo. Comp. 468 (2009) 466-472.

[16] X. Yang, R. Wang, Z. Yang, S. Xu, Structure and properties of Ge–Sb–S–CsCl glass–ceramics, J. Mater. Chem. Phys. 147 (2014) 545-549.

[17] J.Y. Hao, H.T. Liu, Fabrication and Microstructure of Ge-Sb-S-CsCl Chalcogenide Glass Containing β-GeS_2 Nanocrystals, J. Appl. Mech. Mater. 665 (2014) 119-123.

[18] J. Bicerano and S.R. Ovshinsky, Chemical bond approach to the structures of chalcogenide glasses with reversible switching properties, J. non-cryst. Sol. 74 (1985) 75-84.

[19] M. Nunoshita, H. Arai, Energy-band gap and density of Si-As-Te amorphous semiconductors, J. Sol. Stat. Commun. 11 (1972) 337-341.

[20] X. Zhao, N. Long, X. Sun, G. Yin, Q. Jiao, X. Liu, S. Dai and C. Lin, Relationship between composition, crystallization, and phase separation behavior of GeS_2–Sb_2S_3–CsCl chalcogenide glasses, J. Infra. Phys. Tech. 102 (2019) 102978.

[21] I. Kebaili, I. Boukhris, R. Neffati, S. Znaidia, Y.B. Saddeek, K. Aly, A. Dahshan, Theoretical characterization and band gap tuning of $Sn_x(GeSe_2)_{100-x}$ thin films, J. Mater. Chem. Phys. 251 (2020) 123133.

[22] S. Bingol, B. Erdinc and H. Akkus, Optimization, Electronic band structure, optical, dynamical and thermodynamic properties of cesium chloride (CsCl) from first-principles, Int. J. Simul. Multisci. Des. Optim. 6 (2015) A7.

[23] V. Mitsa, R. Holomb, M. Veres, A. Marton, I. Rosola, I. Fekeshgazi, M. Koós, Non-linear optical properties and structure of wide band gap non-crystalline semiconductors, Phys. Stat. Sol. (c), 8 (2011) 2696-2700.

[24] A. Andriesh, M. Iovu and S. Shutov, Optical and Photoelectrical Properties of Chalcogenide Glasses, Chapter in the book: Semiconducting chalcogenide glass III, 80, pp.117-199, Eds: Robert Fairman, beaverton, USA & Boris Ushkov, ELMA, Moscow, Russia, Elsevier Ins., ISBN 0-12-752189-5, 2004.

[25] A. Dahshan and K. Aly, Characterization of new quaternary chalcogenide As–Ge–Se–Sb thin films, J. Philos. Magaz. 88 (2008) 361-372.

[26] A.S. Hassanien and I. Sharma, Band-gap engineering, conduction and valence band positions of thermally evaporated amorphous Ge_{15-x} Sb_x Se_{50} Te_{35} thin films: Influences of Sb upon some optical characterizations and physical parameters, J. All. Comp., 798 (2019) 750-763.

[27] M. Askari, N. Soltani, E. Saion, W.M.M. Yunus, H. Maryam Erfani, M. Dorostkar, Structural and optical properties of PVP-capped nanocrystalline $Zn_xCd_{1-x}S$ solid solutions, Superlatt. Microstruct., 81 (2015) 193-201.

[28] R. Xie, J. Su, Y. Liu, L. Guo, Optical, structural and photoelectrochemical properties of $CdS_{1-x}Se_x$ semiconductor films produced by chemical bath deposition, Int. J. Hydro. Ene. 39 (7) (2014) 3517-3527.

[29] C. Xing, Y. Zhang, W. Yan, L. Guo, Band structure-controlled solid solution of $Cd_{1-x}Zn_xS$ photocatalyst for hydrogen production by water splitting, Int. J. Hydro. Ene. 31 (14) (2006) 2018-2024.

[30] N.N. Greenwood, A. Earnshaw, Chemistry of the Elements, Elsevier 2012.

[31] A. Ammar, A. Farid and S. Fouad, Optical and other physical characteristics of amorphous Ge–Se–Ag alloys, Phys. B: Cond. Matt. 307 (2001) 64-71.

[32] A. Dahshan, K. Aly, Characterization of new quaternary $Ge_{20}Se_{60}Sb_{20-x}Ag_x$ (0≤ x≤ 20 at.%) glasses, J. Non-Cryst. Sol. 408 (2015) 62-65.

[33] H. Hegazy, A. Dahshan and K. Aly, Influence of Cu content on physical characterization and optical properties of new amorphous Ge–Se–Sb–Cu thin films, J. Mater. Res. Expr. 6 (2018) 025204.

[34] L. Jiang, A. Fitzgerald, M. Rose, K. Christova and V. Pamukchieva, X-ray photoelectron spectroscopy studies of thin GexSb40− xS60 chalcogenide films, J. Non-Crys. Sol. 297 (2002) 13-17.

[35] A. Dahshan and H.H. Amer, Physical and optical properties of amorphous $Ge_xAs_{20}S_{80-x}$ thin films, J. Philos. Mag. 91 (2011) 787-797.

[36] I. Sharma, S. Tripathi and P. Barman, Effect of Bi addition on the optical behavior of a-Ge–Se–In–Bi thin films, J. Appl. Surf. Sci. 255 (2008) 2791-2795.

[37] G. Saffarini, J. Saiter, H. Schmitt, The composition dependence of the optical band gap in Ge–Se–In thin films, J. Opt. Mater. 29 (2007) 1143-1147.

[38] V. Pamukchieva, A. Szekeres, K. Todorova, M. Fabian, E. Svab, Z. Revay, L. Szentmiklosi, Evaluation of basic physical parameters of quaternary Ge–Sb-(S, Te) chalcogenide glasses, J. Non-Crys. Sol. 355 (2009) 2485-2490.

[39] J.C. Phillips and M.F. Thorpe, Constraint theory, vector percolation and glass formation, Solid State Commun., 53 (1985) 699-702.

[40] V. Pamukchieva, A. Szekeres, K. Todorova, M. Fabian, E. Svab, Z. Revay, L. Szentmiklosi, Evaluation of basic physical parameters of quaternary Ge–Sb-(S, Te) chalcogenide glasses, Journal of non-crystalline solids, 355 (2009) 2485-2490.

[41] J.C. Phillips, Topology of covalent non-crystalline solids I: Short-range order in chalcogenide alloys, J. Non-Crys. Sol. 34 (1979) 153-181.

[42] M.F. Thorpe, Continuous deformations in random networks, J. Non-Crys. Sol. 57 (1983) 355-370.

[43] S.R. Ovshinsky and D. Adler, Local structure, bonding, and electronic properties of covalent amorphous semiconductors, J. Contem. Phys. 19 (1978) 109-126.

[44] S. Fouad, On the glass transition temperature and related parameters in the glassy Ge_xSe_{1-x} system, Phys. B: Cond. Matt. 293 (2001) 276-282.

[45] H. Ma, X. Zhang and J. Lucas, Infrared transmitting chalcogenide glass ceramics, J. Non-Crys. Sol. 317 (2003) 270-274.

[46] S. El-Sayed, H. Saad, G. Amin, F. Hafez and M. Abd-El-Rahman, Physical evolution in network glasses of the Ag–As–Te system, J. Phys. Chem. Sol. 68 (2007) 1040-1045.

[47] A.V. Kolobov, P. Fons and J. Tominaga, Local instability of p-type bonding makes amorphous GeTe a lone-pair semiconductor, Phys. Rev. B, 87 (2013) 155204.

[48] P. Sharma, Glass-forming ability and rigidity percolation in SeTePb lone-pair semiconductors, Appl. Phys. A. 122 (2016) 402.

[49] L. Tichý, H. Ticha, On the chemical threshold in chalcogenide glasses, J. Mater. Lett. 21 (1994) 313-319.

[50] L. Tichý and H. Ticha, Covalent bond approach to the glass-transition temperature of chalcogenide glasses, J. Non-Crys. Sol. 189 (1995) 141-146.

[51] L. Pauling, The nature of the chemical bond, Cornell university press, New York, 1960.

[52] L. Tichý, A. Tříska, H. Ticha, M. Frumar and J. Klikorka, The composition dependence of the gap in amorphous films of Si_xGe_{1-x}, Sb_xSe_{1-x} and As_xTe_{1-x} systems, J. Sol. Stat. Commun. 41 (1982) 751-754.

[53] A. Pattanaik and A. Srinivasan, Electrical and optical properties of amorphous $Pb_xIn_{25-x}Se_{75}$ films with a dispersion of nanocrystallites, J. Opto. and Adv. Mater. 5 (2003) 1161-1167.

[54] R. Almeida, C. Bocker and C. Rüssel, Size of CaF_2 crystals precipitated from glasses in the $Na_2O/K_2O/CaO/CaF_2/Al_2O_3/SiO_2$ system and percolation theory, J. Chem. Mater. 20 (2008) 5916-5921.

[55] C. Bocker and C. Rüssel, Self-organized nano-crystallisation of BaF_2 from $Na_2O/K_2O/BaF_2/Al_2O_3/SiO_2$ glasses, J. Euro. Ceram. Soc. 29 (2009) 1221-1225.

Funding (Mentioned in the acknowledgement)

Conflicts of interest/Competing interests (There is no conflict of interest)

Availability of data and material (All data were mentioned in the manuscript)

Code availability (Not applicable)

Authors' contributions (All authors contributed equally)

Ethics approval (Not applicable)

Consent to participate (Not applicable)

Consent for publication (Not applicable)

Figures

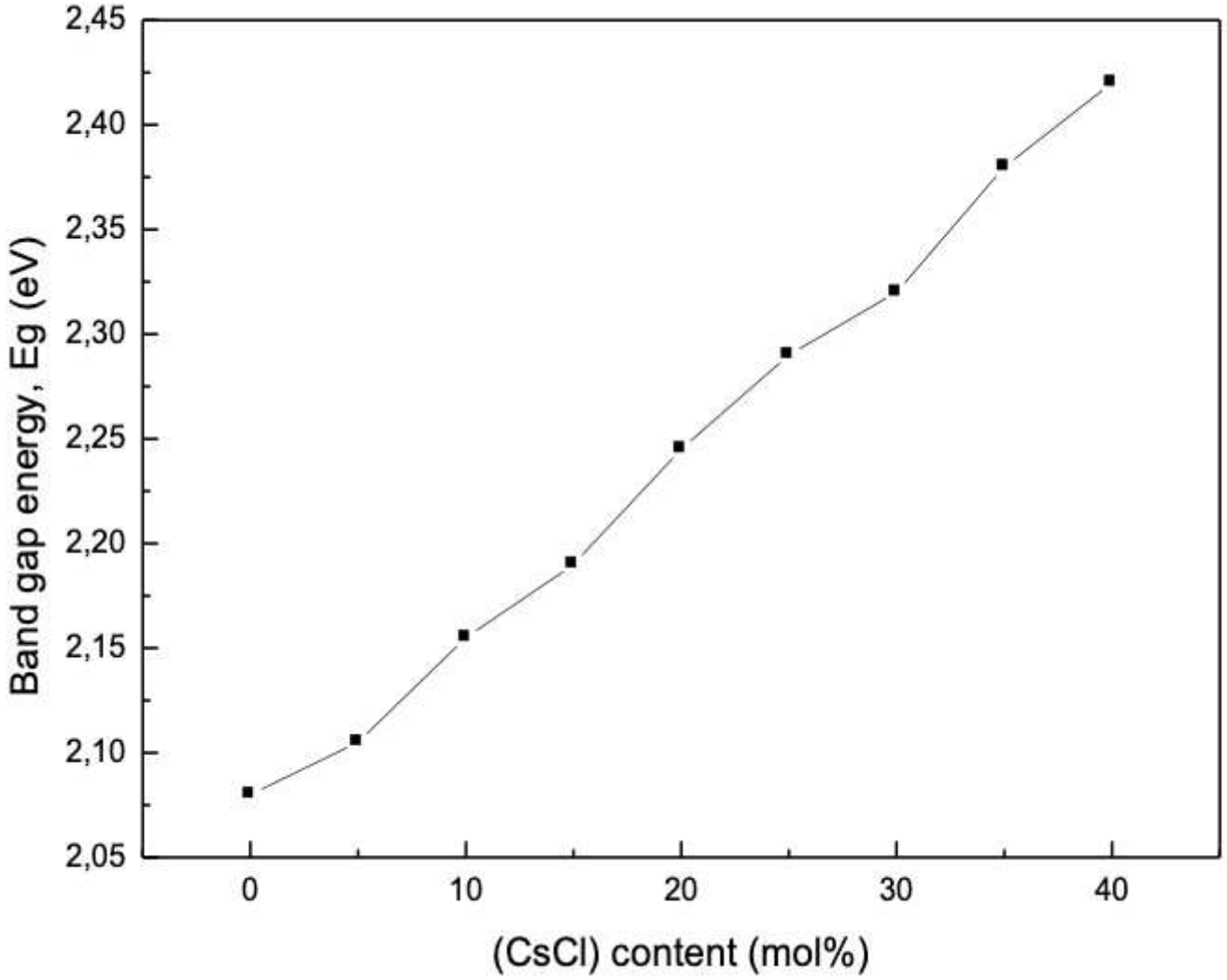

Figure 1

Band gap estimation for (GeS2-Sb2S3)100-x(CsCl)x system

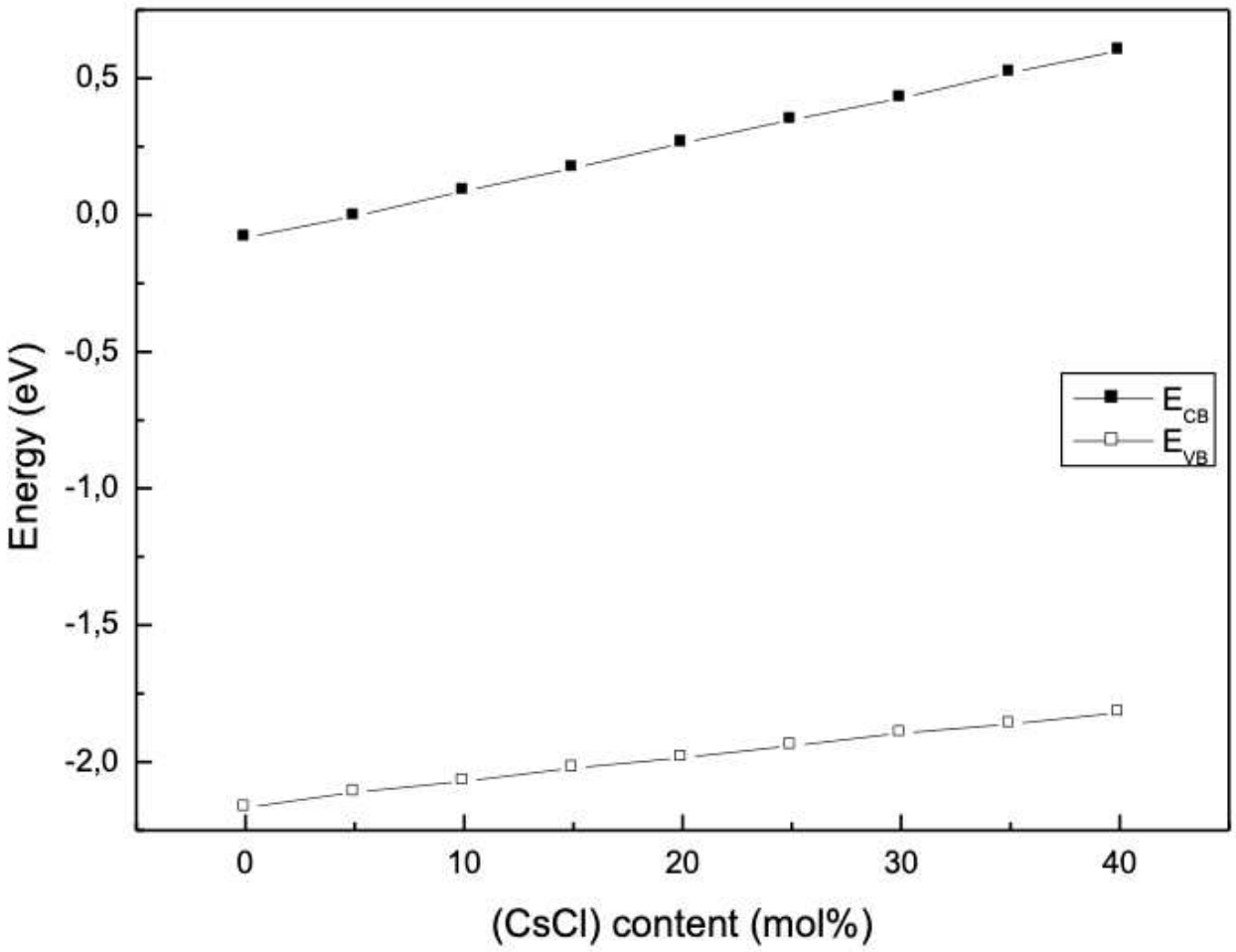

Figure 2

Plots of ECB and EVB against the (CsCl) content for the (GeS2-Sb2S3) 100-x(CsCl)x system

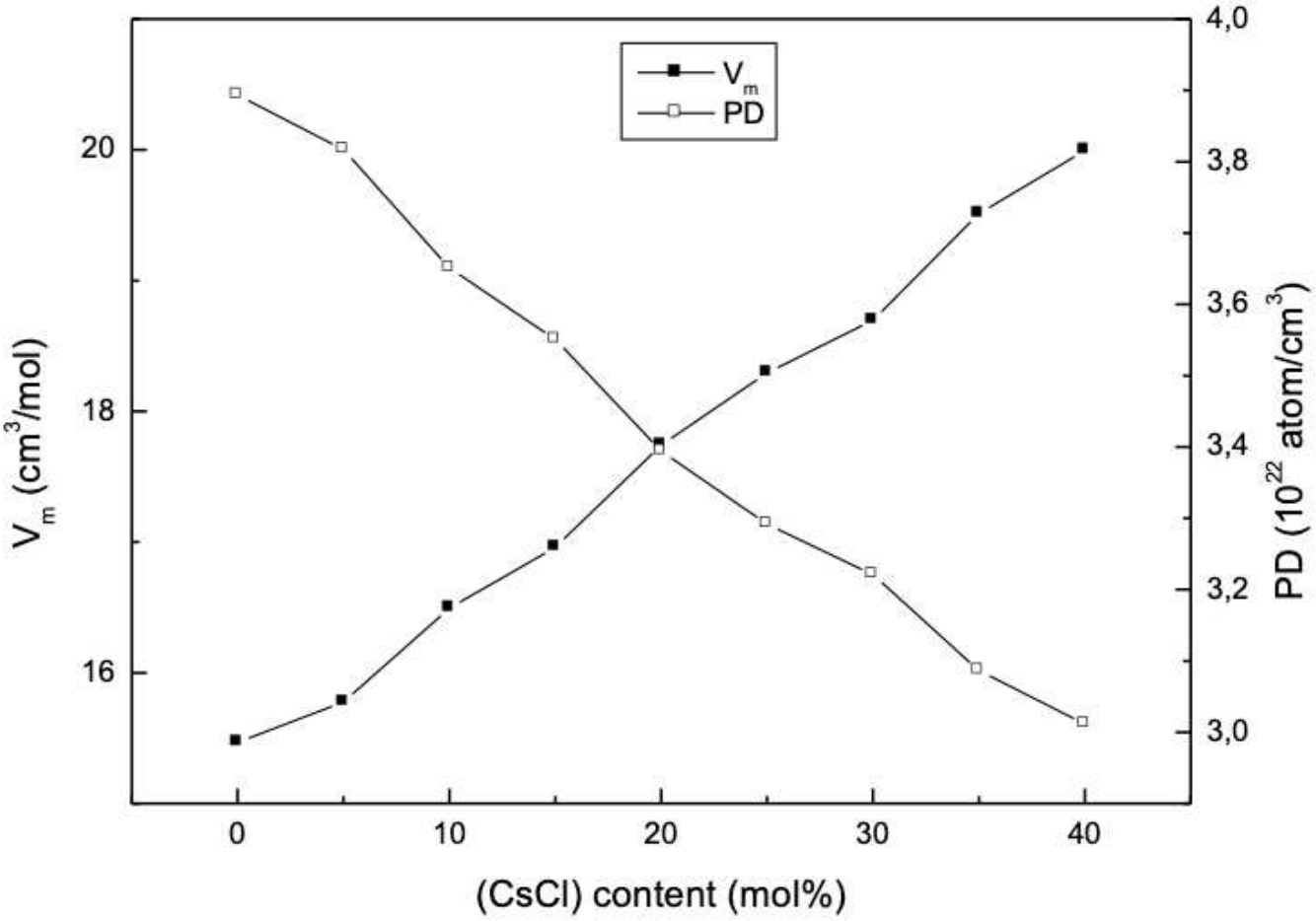

Figure 3

Plots of Vm and PD against the (CsCl) content for the (GeS2-Sb2S3) 100-x(CsCl)x system

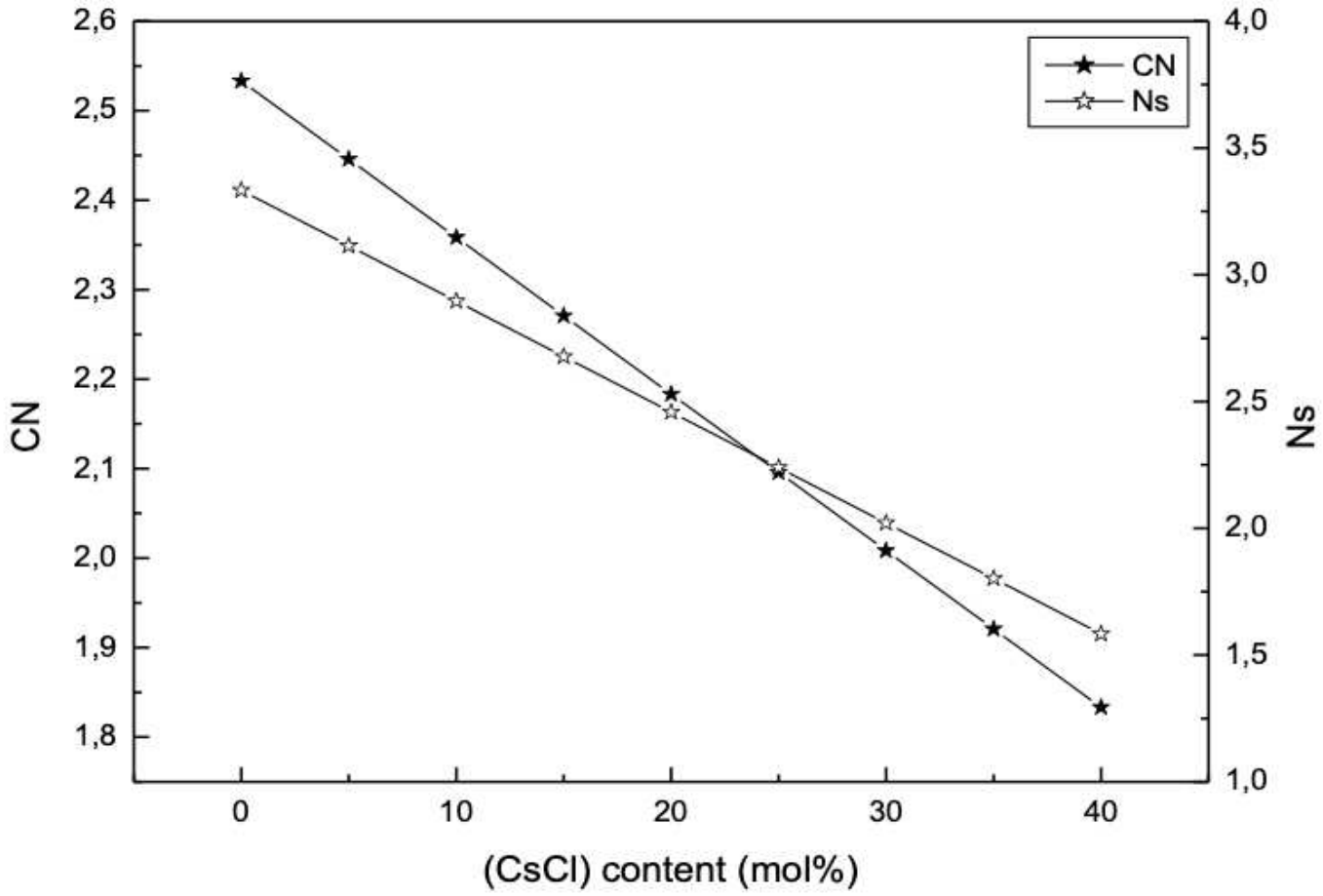

Figure 4

Plots of CN and Ns against the (CsCl) content for the (GeS2-Sb2S3)100-x(CsCl)x system

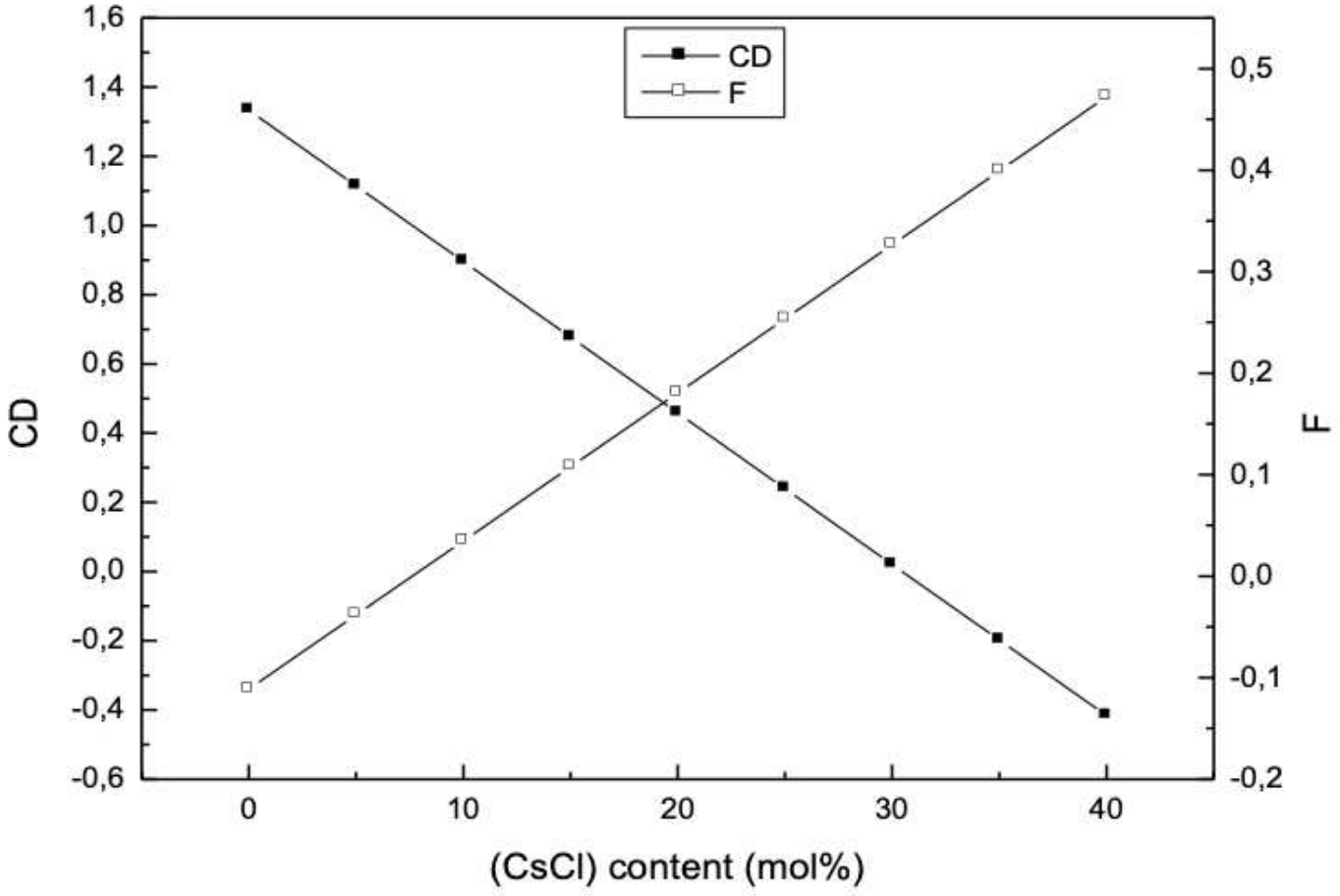

Figure 5

Plots of CD and F against the (CsCl) content for the (GeS2-Sb2S3) 100-x(CsCl)x system

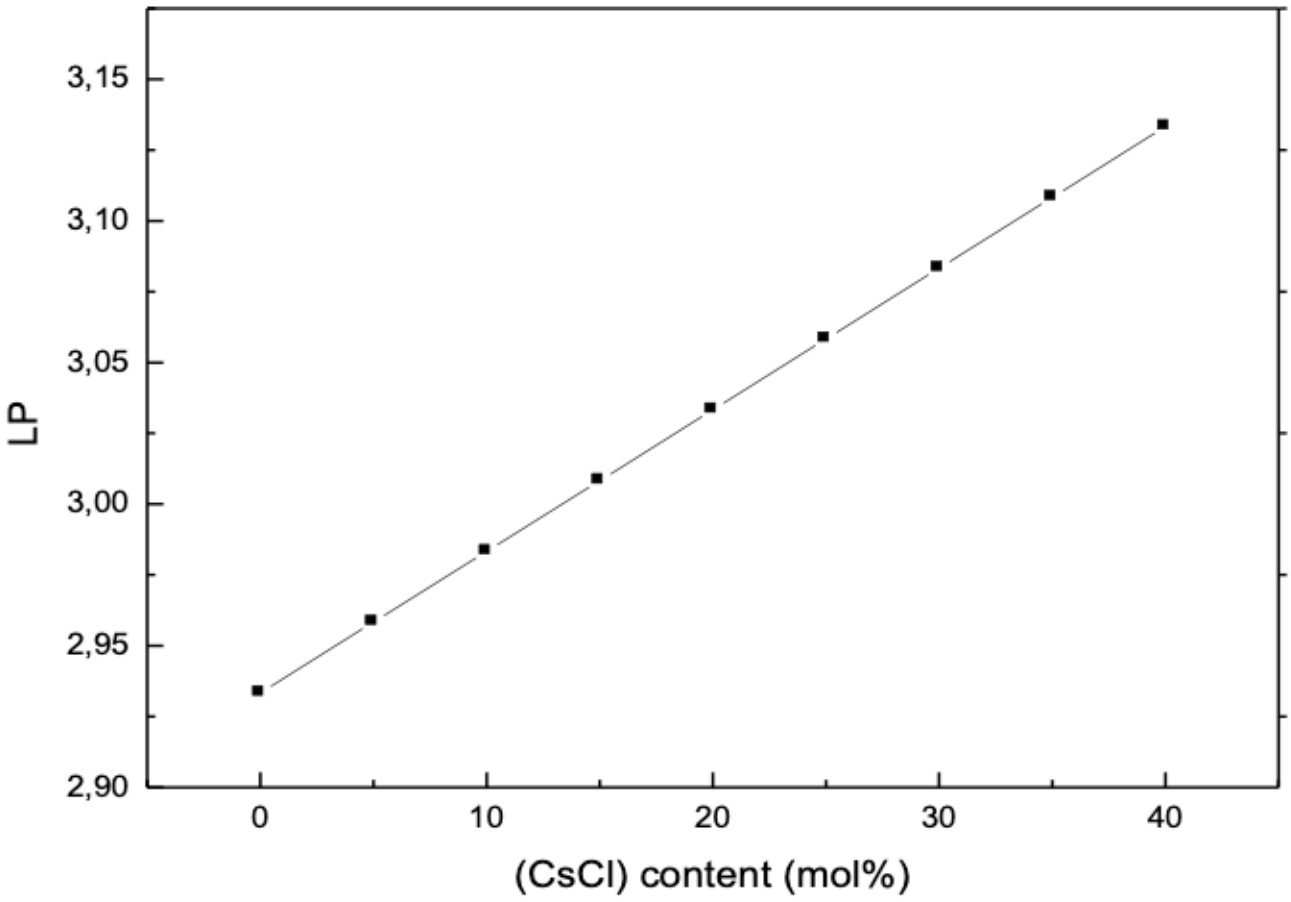

Figure 6

Variation of LP with (CsCl) content in (GeS2-Sb2S3) 100-x(CsCl)x system

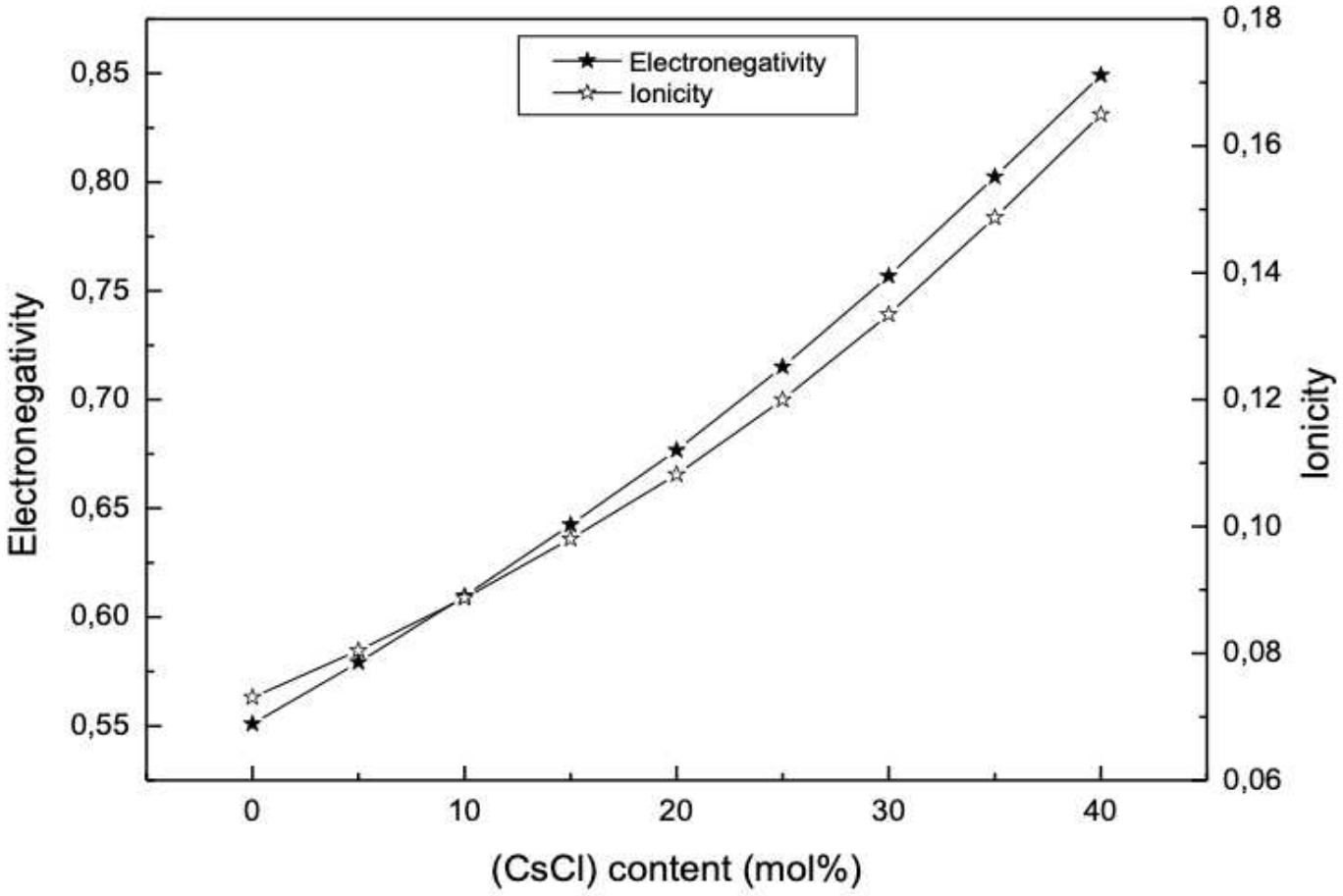

Figure 7

Plots of Δχ and Ion against the (CsCl) content for the (GeS2-Sb2S3) 100-x(CsCl)x system

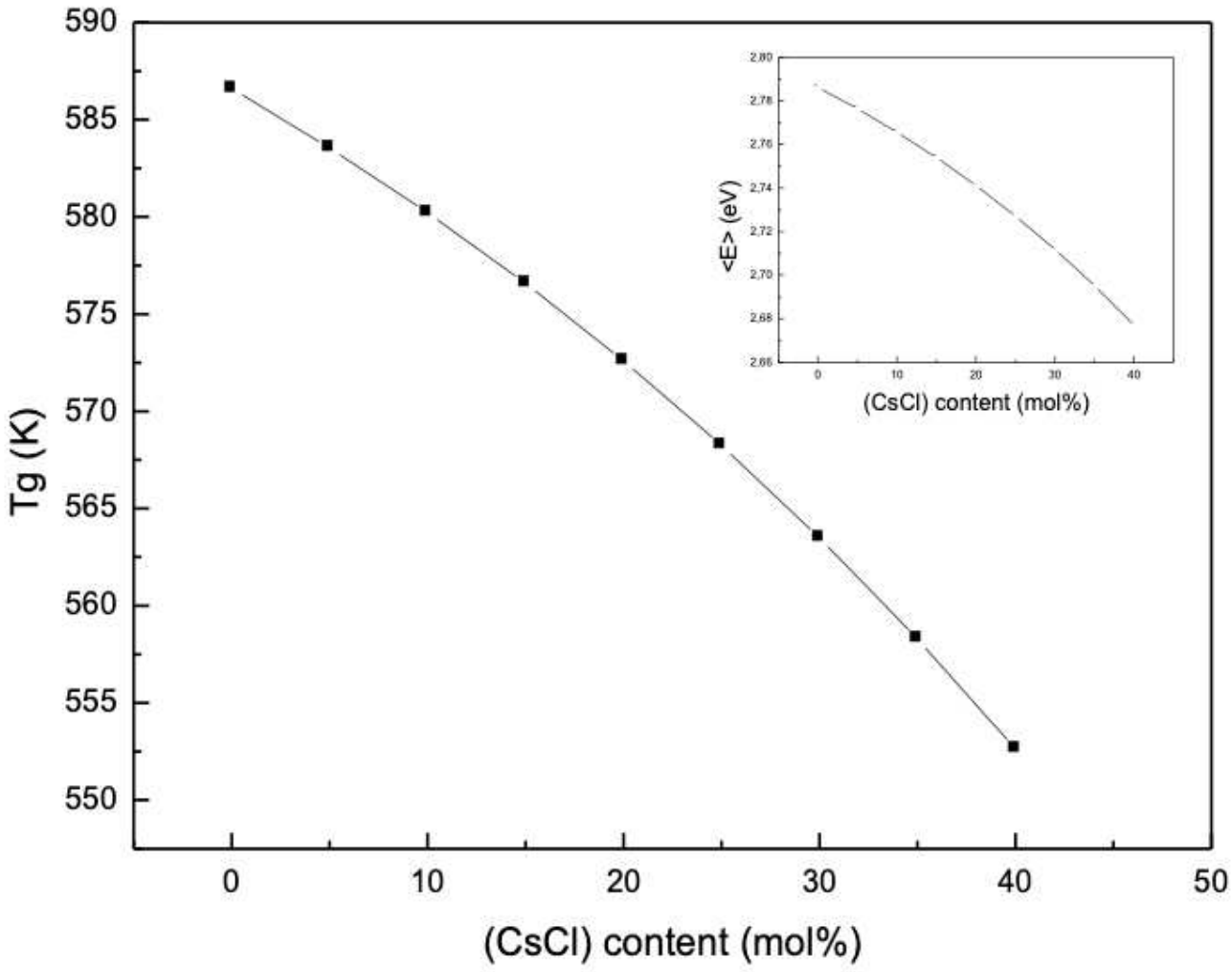

Figure 8

Variation of Tg with the (CsCl) content in the (GeS2-Sb2S3) 100-x(CsCl)x system